INVESTIGATION OF EC CURRENT DRIVE IN A HIGH ELECTRON TEMPERATURE PLASMA IN JT-60U

T. Suzuki[1], *S. Ide*[1], *K. Hamamatsu*[1], *C. C. Petty*[2], *L. L. Lao*[2], *A. Isayama*[1], *T. Fujita*[1], *Y. Ikeda*[1], *M. Seki*[1], *S. Moriyama*[1], *and the JT-60 Team*[1]

[1] Japan Atomic Energy Research Institute, Naka, Ibaraki 311-0193, Japan
[2] General Atomics, San Diego, California, USA

e-mail: suzukit@fusion.naka.jaeri.go.jp

Recent progress in the development of electron cyclotron heating/current drive systems in regard to power and pulse duration have allowed the extension of two normalized parameters (toroidal electric field E_ϕ and wave power density p). In the extended regime, the conventional theory requires consideration of a distorted electron distribution function. The first validation of the ECCD theory in the extended regime having large E_ϕ and p is presented. Linear calculation has a tendency to overestimate the EC driven current, as normalized parameters for E_ϕ and p increase. While the EC driven current I_{EC} obtained by a linearized Fokker-Planck calculation (1.1MA) did not agree with the measured EC driven current (0.74 ± 0.06MA), non-linear calculation of the Fokker-Planck equation considering the effect of E_ϕ (0.76MA) shows close agreement with the experimental result. Calculations show that the decreasing effect of E_ϕ on I_{EC} was stronger than the increasing effect of p on I_{EC} in the experiment.

1 Introduction

Current drive by means of electron cyclotron (EC) waves has been considered effective in a spatially localized control of current profile, because the absorption location of the EC waves is determined mainly by the cyclotron resonance layer and by a controllable injection angle of the waves. Such spatially localized EC driven current has been measured in the DIII-D and in the JT-60U [1]. Control of the electron cyclotron current drive (ECCD) has been used to achieve a high performance plasma. For example, an increase of the normalized beta β_N was observed by stabilizing neo-classical tearing modes (NTM), when the ECCD compensates for a missing bootstrap current produced by the flattening of the plasma pressure profile in magnetic islands [2]. While the ECCD has been used to control the plasma current profile, validation of ECCD theory is currently underway; previous attempts have been made under the condition in which the effects of the distortion of the electron distribution function f_e is smaller than the effect of collision relaxation [1,3]. Such a distortion effect is expected to be seen in the toroidal electric field of a tokamak discharge, and in an oscillating RF electric field by EC waves. In a weak distortion regime, the electron distribution function will be close to the Maxwellian so that linear treatment of the Fokker-Planck equation without taking into account the electric field can be sufficient under this condition.

Recent progress in the development of EC systems in JT-60U enabled us to do experiments in which the regime was extended under well-diagnosed conditions [4]. As will be described later, the regime is represented by two physical parameters, that is, a normalized toroidal electric field and a normalized wave power density. The parameters in the JT-60U are about 8 (for the normalized toroidal electric field) and 5 (for the normalized wave power density) times larger than those in the DIII-D [3,5], which is one of devices in which intensive study on validation of the ECCD theory is being conducted. Theoretical works have suggested that the relaxation effect induced in an electron by collision is represented by electron density n_{e19} against heating power per an electron p/n_{e19}, and by the critical electric field producing run-away electrons E_{cr} against toroidal electric field E_ϕ. The power density p is measured in MWm^{-3} and electron density in $10^{19}m^{-3}$ units. Thus, the normalized parameters are p/n_{e19}^2 for wave power density p, and E_ϕ/E_{cr} for toroidal electric field E_ϕ, respectively. We employ a formalism of Knoepfel for E_{cr} as defined in reference [6]. The formalism takes into account the effective charge by impurity ions.

An increase in the EC heating power, which is proportional to square of the RF electric field, leads to an increase in absorption power, and hence absorption power density p. This extended the parameter p/n_{e19}^2, along with low electron density achieved by conditioning the first wall in order to reduce recycling. The strong electron heating by the EC waves produces an increase in electron temperature T_e above 20keV. The high T_e and the low n_e reduce E_{cr}. A large EC driven current induces a large Ohmic toroidal electric field, which becomes even negative just after the start of the ECCD. The high T_e, low n_e and large EC driven current extend the absolute value of E_ϕ/E_{cr}. The increased EC power increases both the parameters simultaneously. Sufficiently longer pulse duration of EC waves than duration required for analysis (typically, at least 0.6s: 0.1-0.2s for T_e raise and 0.4s for the analysis) enabled us to measure the EC driven current profile and the toroidal electric field profile in the plasma, which are important physical quantities in this study.

In the present study, we examine ECCD theory in the extended E_ϕ/E_{cr}-p/n_{e19}^2 regime. We compare the EC driven current measured in the experiment to results predicted by the linear or the non-linear theory, and discuss the effect of the distortion of the distribution function on the ECCD. Section 2 describes the experimental measurement of the EC driven current profile and the toroidal electric field profile. Comparison of the experimental results with theoretical calculations will be made in section 3. A summary is provided in section 4.

2 Experiment

The EC driven current profile and the toroidal electric field profile have been evaluated by the analysis of the loop voltage profile [1]. We briefly describe this

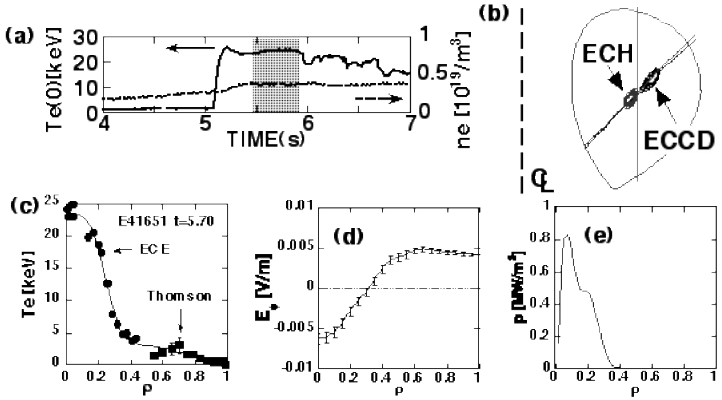

Figure 1: (a) temporal evolution of electron temperature at the plasma center $T_e(0)$ and of line averaged electron density n_e. EC injection starts at t=5.1s. (b) poloidal cross-section of the plasma with EC ray trajectories and with the absorbed locations of EC waves. A vertical line represents the cyclotron resonance for cold electrons. Two locations (ECH/ECCD) respectively represent absorbed locations of vertically/obliquely injected EC waves to the toroidal direction. Absorption power was 0.6MWfor the ECH and 2.3MWfor the ECCD. (c) electron temperature profile measured by ECE and by Thomson scattering. (d) measured toroidal electric field profile $E_\phi(\rho)$ with errors in the period shown by the hatched region in (a). (e) absorbed power density profile $p(\rho)$ by a linearized Fokker-Planck code.

analysis. Poloidal magnetic flux profiles are determined by the reconstruction of magnetic equilibrium using internal magnetic field measured by motional Stark effect (MSE) polarimetry [7]. The toroidal electric field profile $E_\phi(\rho)$ can be calculated by the temporal derivative of the poloidal magnetic flux profiles (Faraday's law). Here, ρ is the normalized minor radius. The Ohmic current density profile is assumed to be a product of the neo-classical conductivity σ_{NC} and the toroidal electric field. Since the total toroidal current profile has already been calculated by the equilibrium reconstruction, subtraction of the Ohmic current profile $\sigma_{NC}E_\phi$ from the total current profile leads to a non-inductive current profile. By subtracting the calculated bootstrap current and beam driven current from the non-inductive current, we obtain the EC driven current profile $j_{EC}(\rho)$. Although both the bootstrap current density and the beam driven current density are small in the following experiments, compared to the Ohmic current density, they have been numerically calculated. The EC driven current I_{EC} is the integration of j_{EC} over the plasma poloidal cross-section.

Here we see a discharge having the largest E_ϕ/E_{cr} and p/n_{e19}^2 in this study. Figure 1(a) shows the temporal evolution of the central electron temperature $T_e(0)$ and the line averaged electron density n_e. After the start of 2.9MW of EC injection at t = 5.1s, $T_e(0)$ increases to 23keV and is sustained for about 0.8s. The optical thickness was more than 30 around the plasma's center, so that we expect that the radiation temperature represents the electron temperature. The slight increase in n_e is due to an increased fueling by the diagnostic neutral beam for the MSE diagnostic. The loop voltage profile analysis described above was made in the period indicated by the hatched region (t =5.5-5.9s) in Fig. 1(a). The poloidal cross-section of the plasma containing ray-trajectories of EC waves is shown in Fig. 1(b). We employed a combination of the ECH and the ECCD to sustain the high T_e long enough to analyze the loop voltage profile. Figure 1(b) also shows the deposition locations for the ECH and the ECCD calculated using the ray-tracing method. The electron temperature profile during the ECCD analysis is shown in Fig. 1(c). Figure 1(d) shows the evaluated E_ϕ profile by the loop voltage profile analysis. The parameter E_ϕ/E_{cr} reached -1.7% at the plasma center. The positive direction of E_ϕ is the same as that of the plasma current and co-ECCD. We must note that E_ϕ can vary in time. The time scale of the change of E_ϕ is about τ_R=22s, where τ_R is a local resistive diffusion time for j_{EC} width (0.16m). Since τ_R is quite longer than the duration of the analysis (0.4s), E_ϕ changes little during the analysis. In addition, since the momentum deflection time of a test electron τ_{de} is about 0.16s, E_ϕ is steady against the distortion of the electron distribution function. Calculated absorbed power density p is shown in Fig. 1(e). The parameter p/n_{e19}^2 was 4.9 at the peak of p. The EC driven current density profile $j_{EC}(\rho)$ determined by the loop voltage profile analysis is shown by the solid curve in Fig. 2(a). The corresponding result obtained by a linearized calculation (described later) using the experimental parameters is represented by a dotted curve. The measured j_{EC} profile is spatially localized, showing no significant radial diffusion of current density compared to the linear calculation. Errors in the experimental j_{EC} come mainly from errors in Ohmic current $\sigma_{NC}E_\phi$, where the error in E_ϕ is shown in Fig. 1(d). Error in σ_{NC} is 15% of σ_{NC} due to the error in T_e of 10%. Figure 2(b) shows the EC driven current profile $I_{EC}(\rho)$ enclosed in a magnetic surface at a normalized minor radius ρ. While the total measured I_{EC} is 0.74MA, the linear calculation predicts 1.1MA, overestimating the I_{EC} by 48%.

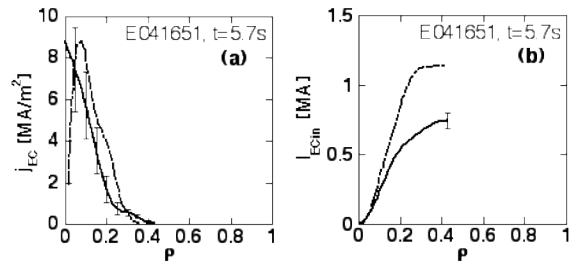

Figure 2: (a) EC driven current density profiles j_{EC} in the experiment (solid curve) and in the linearized calculation (dotted curve). Measured j_{EC} is spatially localized, showing no significant radial diffusion of current density. (b) EC driven current enclosed in a magnetic surface at ρ.

3 Analysis

Brief descriptions of Fokker-Planck codes are provided first, followed by a comparison of the experimental results to the calculation results. In this study, we employs two codes to calculate the EC driven current profile; a linear code without E_ϕ (RADAR code) and a non-linear code with E_ϕ (CQL3D code [8]). The common physics included shared by both of the codes are

1. wave propagation by ray-tracing
2. toroidal geometry with trapped particles
3. relativistic effect
4. momentum conservation in not only electron-ion collisions, but also in electron-electron collisions.
5. a quasi-linear diffusion operator by waves
6. a steady solution of the Fokker-Planck equation; $\partial f/\partial t = 0$
7. neglect of radial diffusion

The last item is validated by the experimental result shown in Fig. 2, as described in section 2. While the RADAR code quickly solves the Fokker-Planck equation without the toroidal electric field by linearizing the electron distribution function f_e, the CQL3D code directly solves the Fokker-Planck equation numerically. While only one minute of calculation is required by the RADAR code, the CQL3D calculation requires 12 hours. The RADAR code has an advantage to be run within shot intervals in experiment. The non-linear calculation is considered to converge to the linearized calculation under a limit of zero EC wave power, when $E_\phi = 0$.

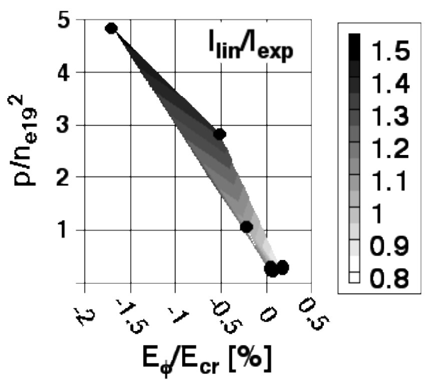

Figure 3: Contour plot of I_{lin}/I_{exp} on an E_ϕ/E_{cr}-p/n_{e19}^2 plane. Both the parameters (E_ϕ/E_{cr}, p/n_{e19}^2) are almost linearly coupled, since a strong negative electric field requires a larger EC driven current, and hence larger ECCD power. Data within $|E_\phi/E_{cr}| < 0.22$ and $p/n_{e19}^2 < 1$ show agreement between linear calculations and measurements. Linearized calculation tends to overestimate the EC driven current than the experiment, when $-E_\phi/E_{cr}$ and p/n_{e19}^2 increases. Overestimation by 48% is seen for the largest I_{lin}/I_{exp}.

We investigated the total EC driven current in linear calculation (I_{lin}) normalized by that in the experiment (I_{exp}); I_{lin}/I_{exp}. Figure 3 shows a contour plot of I_{lin}/I_{exp} on E_ϕ/E_{cr}-p/n_{e19}^2 space. While p is evaluated by the linear calculation, other parameters are based on measurement. The absolute value of E_ϕ/E_{cr} increased along with an increase of p/n_{e19}^2 in the experiment so that they are almost linearly coupled. A contour plot of I_{lin}/I_{exp} shows a tendency to decrease with an increase in the absolute value of negative E_ϕ/E_{cr}, and with an increase of p/n_{e19}^2. The EC driven current in linear calculation agrees with experimental result within errors in measurement, under conditions $p/n_{e19}^2 < 1$, and $|E_\phi/E_{cr}| < 0.22\%$. The ratio I_{lin}/I_{exp} increased up to 1.48, showing over-estimation by the linearized calculation, in the case of $p/n_{e19}^2 \sim 4.9$ and $E_\phi/E_{cr} \sim -1.7\%$. The dynamic ranges of both parameters in this study were 8 times larger than that in the DIII-D [3,5] for E_ϕ/E_{cr} and 5 times larger for p/n_{e19}^2, as was reported previously [4]. The large discrepancy between the experiment and the linear calculation has been first observed in this experiment. Thus, this experiment can be a good touchstone of both the non-linear effect and the E_ϕ effect, even if they are coupled.

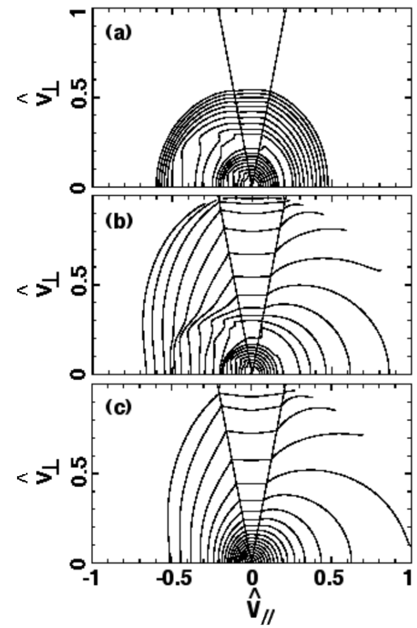

Figure 4: Distribution function of electrons f_e at ρ=0.08 calculated by the non-linear Fokker-Planck code (CQL3D). (a) ECCD at E_ϕ=0. (b) ECCD at measured E_ϕ profile. (c) measured E_ϕ field without ECCD. The two lines in each figure show the boundary for trapped particles at ρ=0.08.

It has been reported that a negative toroidal electric field reduces the CD efficiency compared to that without a toroidal electric field [9], and that non-linear calculation predicts larger CD efficiency than does linear calculation [10]. The above experimental result can be explained by both the toroidal electric field effect and the non-linear effect, assuming a stronger toroidal electric field effect than a non-linear one. Thus we performed non-linear calculations using the CQL3D code. Figure 4 shows the contour plots of the distribution function of electron f_e for various cases under the experimental condition in Fig. 2; (a) ECCD at E_ϕ=0, (b) ECCD at the measured E_ϕ profile, (c) the measured E_ϕ field without ECCD. We see f_e at the radial location of ρ=0.08 where the absorption power density by the CQL3D peaks and E_ϕ is negatively large (see Fig. 1(d)). The horizontal and vertical axes are the parallel and perpendicular components of a normalized velocity $\hat{v}$ to the direction of magnetic field, respectively. The velocity v is defined as momentum per unit rest mass m, and the velocity is normalized by the maximum velocity of the corresponding energy of 3MeV. Thermal electron velocity $(T_e/m)^{0.5}$ corresponds to 0.031 in this figure. Since the toroidal magnetic field and the plasma current are in the same direction in this experiment, perpendicular broadening of f_e at negative $\hat{v}_{//}$ (as seen in Fig. 4(a)) shows an increase of electron current, and hence co-ECCD. Under the limit of zero EC power, the distortion decreases and f_e converges to the Maxwellian.

The EC driven current under the limit will be that obtained by linear calculation.

An effect of E_ϕ can be seen in Fig. 4(c), where no ECCD is applied. Since the electric field at the plasma center is negative to the plasma current direction, the electrons are dragged in the positive direction of $\hat{v}_{//}$. Figure 4(b) shows the combined results of ECCD with E_ϕ. We can see strong distortion of f_e under the experimental condition for the most extreme case seen in Fig. 3. The ECCD effect under E_ϕ field is expressed by the difference between (b) and (c). We must note that the 'ECCD effect' includes a synergic effect of E_ϕ and the RF electric field; electrons scattered by the RF field suffer the E_ϕ field. Since the synergic effect is hard to separate each other, the difference between (b) and (c) is usually called as an 'ECCD effect', in a meaning of current increase by EC application. On the other hand, the true E_ϕ effect on a distorted distribution function (Fig. 4(a)) is clearly defined by the difference between (b) and (a).

The calculated EC driven currents in various conditions are shown in Fig. 5, in comparison with the experimental results (Fig. 2(b)). When we compare the linear calculation without E_ϕ (I_{EC}=1.1MA) to that with E_ϕ (I_{EC}=0.66MA), the EC driven current decreases by a factor of 0.6. The strong decreasing effect by E_ϕ on I_{EC} can also be seen in a comparison of the non-linear calculation with (I_{EC}=0.76MA) /without E_ϕ (I_{EC}=1.2MA). On the other hand, a non-linear power effect can be seen in a comparison of the linear and non-linear calculations. The non-linear effect was smaller than the E_ϕ effect in this experimental condition. Comparing calculations to the experiment with errors (I_{EC}=0.74±0.06MA), non-linear calculation taking into account the E_ϕ best agrees with the experiment. Consideration of both of the non-linear effect and toroidal electric field effect is necessary.

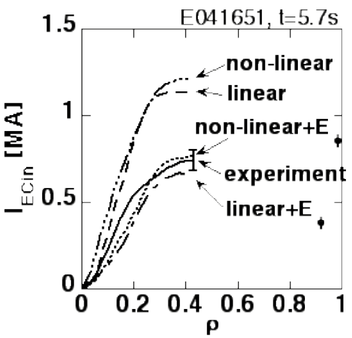

Figure 5: Profiles of EC driven current enclosed in a magnetic surface I_{ECin}. EC driven current obtained by experiment (solid curve) and by various calculations are shown; dashed curve: linear calculation without E_ϕ, dot-dashed curve: linear calculation with E_ϕ, three-dots-dashed curve: non-linear calculation without E_ϕ, dotted curve: non-linear calculation with E_ϕ. Non-linear calculation with E_ϕ agrees the closest with the experimental result concerning to the EC driven current.

The results of this study suggest the accuracy of the EC driven current, and hence the ECCD efficiency η_{CD} is improved by taking account of both the toroidal electric field effect and the non-linear effect. Such an improvement of accuracy in η_{CD} could reduce the power margin of an EC facility necessary to drive a required current, and hence could also reduce the cost, as in the international thermonuclear experimental reactor (ITER), although both the characteristic parameters (E_ϕ/E_{cr}, p/n_{e19}^2) are small in the standard operation in ITER due to high n_e. Consideration of E_ϕ/E_{cr} will be necessary in an advanced start-up scenario without an Ohmic solenoid [11]. In the low n_e condition in the start-up, both the effects will be important to plan the scenario. Predictive analysis for experiments regarding current profile control in which the ECCD is transiently applied to control current, should also consider a transient E_ϕ. Finally, from the view point of ECCD efficiency in ITER, the experimental η_{CD} shown in Fig. 2 can reasonably approach the predicted one in the ITER, as previously explained [4].

4 Summary

Recent progress in the development of electron cyclotron heating/current drive systems in regard to injection power and pulse duration has allowed the extension of two normalized parameters (toroidal electric field E_ϕ/E_{cr} and wave power density p/n_{e19}^2). These parameters have characteristic effects on the distortion of the electron distribution function. In the extended regime, the conventional theory requires consideration of the distorted electron distribution function. We have compared an EC driven current measured experimentally to results predicted by the linear or the non-linear theory. The linear theory without including an electric field has a tendency to overestimate the EC driven current, as absolute value of negative E_ϕ/E_{cr} increases and with increasing p/n_{e19}^2. While the linear calculation without E_ϕ overestimates the EC driven current by a factor of 48% in the most extreme case, non-linear calculation including measured E_ϕ (I_{EC}=0.76MA) agrees closely with the experimental result (I_{EC}=0.74±0.06MA). Electron distribution functions distorted by the non-linear effect and by the E_ϕ effect have been calculated, showing strong distortion of f_e. A comparison of the EC driven current for various calculations has shown that the decreasing effect of the negative E_ϕ on I_{EC} was stronger than the increasing effect of power density, under the experimental conditions.

Acknowledgements

The authors wish to thank members who have contributed to the JT-60 project for their fruitful discussion, and continuous support and encouragement. The authors also wish to thank Dr. R. W. Harvey for his development of the CQL3D code, and for his valuable discussion.

References

[1] T. Suzuki *et al*., Plasma Phys. Control. Fusion **44**, 1 (2002).
[2] A. Isayama *et al*., Plasma Phys. Control. Fusion **42**, L37 (2000).
[3] C. C. Petty *et al*., Nuclear Fusion **42**, 1366 (2002).
[4] T. Suzuki *et al*., to be published in Nuclear Fusion.
[5] C. C. Petty *et al*., Nuclear Fusion **43**, 700 (2003).
[6] H. Knoepfel and D. A. Spong, Nuclear Fusion **19**, 785 (1979).

[7] T. Fujita *et al*., Fusion Eng. and Design **34-35**, 289 (1997).
[8] R. W. Harvey and M. G. McCoy, 1993 Proc. IAEA Technical Committee Meeting (Montreal, 1992) (Vienna: IAEA) p498.
[9] Y. N. Dnestrovskij *et al*., Nuclear Fusion **28**, 267 (1988).
[10] R. W. Harvey *et al*., Phys. Rev. Lett. **62**, 426 (1989).
[11] Y. Takase for the JT-60 Team, "Radio Frequency Power in Plasmas", 15th Topical Conference on Radio Frequency Power in Plasmas (Moran, 2003) (Melville: AIP) p235.